

Contents lists available at ScienceDirect

# **Computers and Chemical Engineering**

journal homepage: www.elsevier.com/locate/cace





# Simultaneous design and operational optimization for flexible carbon capture process using ionic liquids

Kyeongjun Seo, Adhika P. Retnanto, Jorge L. Martorell, Thomas F. Edgar, Mark A. Stadtherr, Michael Baldea\*

McKetta Department of Chemical Engineering, The University of Texas at Austin, Austin, TX 78712, United States

#### ARTICLE INFO

#### Keywords: Carbon capture Flexible operation Ionic-liquid Solvent storage

#### ABSTRACT

Carbon capture and storage is an effective way to abate  $CO_2$  emissions during the transition to zero-carbon power generation technologies. As renewable electricity sources such as wind and solar photovoltaics become more prevalent, conventional power generation systems are increasingly required to operate at highly variable rates in order to balance intermittent renewable power supply. As a result, post-combustion carbon capture systems integrated with fossil fuel power plants must also operate at variable load. In addition, the solvent regeneration and  $CO_2$  compression in capture plants requires substantial amounts of energy and such flexible operation can present an opportunity for operators to take advantage of fluctuating electricity prices, potentially offsetting the cost of carbon capture. This can be achieved through, among others, variable capture rates and utilization of solvent storage. In this paper, we consider a carbon capture system using ionic liquids as a chemical absorption solvent. We study the optimal flexible operation of this system when connected to a natural gas combined cycle power plant under high variable renewable power generation rates. The results show significant cost savings relative to the case of inflexible capture system operation.

## 1. Introduction

The emission of greenhouse gases (GHGs), including carbon dioxide, has been identified as a primary cause of global warming, with fossil fuel-based power plants being a significant contributor to this issue (United States Energy Environmental Protection Agency, 2023). Retrofitting existing power plants with post-combustion carbon capture units is an efficient and cost-effective way to reduce  $\rm CO_2$  emissions (Wu et al., 2014; Zanco et al., 2021). Several technologies for post-combustion carbon capture have been developed, including solvent absorption (Rochelle et al., 2011), membrane-based separation (Kárászová et al., 2020), and solid adsorption (Samanta et al., 2012). Among these technologies, solvent absorption is the most studied and widely implemented in industry (Bui et al., 2018).

In recent years, the amount of electricity generated from renewable sources, including solar photovoltaics (PV) and wind turbines has significantly increased. The share of US power generation from renewable sources is expected to surge from 21% in 2021 to 44% by 2050 (United States Energy Information Administration, 2022a). This shift towards renewable energy is a positive development in terms of reducing GHG emissions and minimizing environmental impacts of the power industry. However, it presents challenges to traditional fossil fuel-based (dispatchable) generation. "Dispatchable" refers to power generation

sources that can be easily turned on and off as needed to match changes in electricity demand on the grid. These sources typically include fossil fuel-based power plants, which can modify (increase or decrease) their output to balance changes in electricity demand. However, high levels of renewable power generation can alter the electricity net-load curve and impact the ability of dispatchable power systems to balance supply and demand on the grid (Hou et al., 2019). PV generation typically peaks during the day, but energy demand typically peaks in the evening when solar PV supply is reduced. Therefore, integrating intermittent generation like wind and PV in the power generation portfolio may force dispatchable power plants to operate on a loadfollowing or cyclic basis, resulting in highly fluctuating output to meet variable loads (Gonzalez-Salazar et al., 2018). In order to make the implementation of carbon capture from power plants both technically and economically viable, the carbon capture process also needs to be capable of accommodating rapid and significant load changes (Rúa et al., 2020).

The energy for solvent regeneration in a carbon capture system is typically provided by low-pressure steam, which can be diverted from the power plant. In addition, compression of captured  ${\rm CO}_2$  requires a significant amount of work, provided by electric motors. High penetration of renewable energy sources can cause volatility in electricity

E-mail address: mbaldea@che.utexas.edu (M. Baldea).

Corresponding author.

prices due to their intermittency and oversupply/curtailment. Fluctuations in demand (often driven by residential users) also cause electricity prices to vary. Thus, the operating cost of a carbon capture system installed at a fossil fuel-fired power plant can be reduced by adjusting its operation in response to the time-varying price of electricity (Bruce et al., 2016; Hao et al., 2020). Specifically, capture rates (and hence the energy used for regeneration and compression) can be reduced during periods of high electricity demand (and hence high price). Conversely, capture rates can be increased when grid electricity demand is low.

In light of the above, flexibility becomes an important consideration when designing and operating carbon capture processes for power plants. Flexibility is promoted by certain design features, such as the capability to adjust the instantaneous capture level over time while ensuring that the operating capture level meets, on average, over a specified time, a given target value (typically 90% of  $\rm CO_2$  fed to the capture process), and the ability to store lean and rich  $\rm CO_2$ -absorbing solvent (Errey et al., 2014; Bui et al., 2014; Cohen et al., 2012; Spitz et al., 2019; Chalmers et al., 2009). The flexibility benefits of such features can be explained as follows:

- The instantaneous capture level refers to the real-time percentage of CO<sub>2</sub> captured relative to CO<sub>2</sub> produced by the power plant and fed to the capture unit in the flue gas. Allowing for variable instantaneous capture levels provides flexibility in response to the grid status. In periods of peak power demand, the instantaneous capture rate can be decreased to minimize energy consumption, which is typically diverted from power generation low-pressure steam and utilized for solvent regeneration. This can be achieved by either reducing the rate of solvent regeneration or reducing the amount of steam used, which will result in a richer CO2 loading (higher CO<sub>2</sub> content) of the regenerated solvent. This can be especially advantageous when the power demand on the grid is high. Conversely, during periods of low power demand, the instantaneous capture rate can be increased beyond the design value to offset the decrease in the capture rate during peak demand periods.
- The solvent storage system comprises two tanks: a rich storage tank, which collects the solvent as it exits the absorber before it is regenerated, and a lean storage tank, which collects the lean solvent after regeneration. The purpose of these tanks is to make the operation of the combined power plant and carbon capture system more flexible by decoupling the absorption and desorption of CO<sub>2</sub>. For example, the rich solvent is stored during periods of high electricity prices. During off-peak periods, the rich solvent from the storage tank is regenerated.

Other strategies, such as a bypass option (Chalmers et al., 2009; Cohen et al., 2011), can be used. This refers to exhaust gas venting, which involves temporarily disabling the  $CO_2$  capture plant while keeping the power cycle operational. A significant portion of the electricity penalty associated with the carbon capture process can be eliminated. The bypass option may be economically advantageous during periods of high electricity prices. However, this strategy may result in the unabated emission of all the  $CO_2$  produced by the power plant during the bypass period, and excessive bypassing makes it difficult to achieve the desired reduction level (e.g. 90%) in long-term time-averaged emissions. Therefore, this option is not considered in this work.

Previous research on post-combustion carbon capture systems initially focused on a fixed load operation, with a constant flow of flue gas treated through the capture system. This means that the power plant is operating at a fixed load while the rates of  $\mathrm{CO}_2$  absorption, regeneration and compression in the capture system are constant at all times (Rubin et al., 2007; Jockenhoevel et al., 2009; Plaza et al., 2009; Tsay et al., 2019; Seo et al., 2020). Subsequent studies (Khalilpour, 2014; Bui et al., 2014; Cohen et al., 2011; Cheng et al., 2022; Zantye et al., 2019; Alie et al., 2016) have investigated the flexible operation of

carbon capture systems. However, many of these studies lack thorough consideration of process-level decisions and constraints for the carbon capture process. Although some of the decision variables (e.g., plant load, regeneration load, storage level, capture level) can be varied dynamically in response to fluctuating electricity prices in order to improve the economics of the capture process, they mostly relied on simple linear models relating the process load and the corresponding cost and CO<sub>2</sub> emission level. For example, Cheng et al. (2022) and Zantye et al. (2019, 2021) utilized linear functions to link the partial load of absorption and desorption columns to their energy consumption. Although the linearized models appeared to be accurate, they were based on nominal operating conditions (e.g. operating temperature, pressure, and absorbent CO2 loading), and opportunities for flexibility were limited. Zaman and Lee (2015) developed an equilibrium-based carbon capture process model that incorporated solvent storage and variable capture rate as flexibility-enabling components. However, the operating conditions, such as absorption and regeneration temperatures, were fixed throughout the day, and the objective function did not consider detailed capital investment costs, including absorber and storage size, and were not optimized simultaneously. The overall process economics of carbon capture systems are represented nonlinearly by the combinations of different operating conditions, such as temperature and compression load, which need to be optimized simultaneously to achieve maximum cost efficiency.

Motivated by the above, we propose an optimization framework for the design and operation of a flexible carbon capture plant. A detailed rate-based, process-level representation of the post-combustion carbon capture plant is developed. We simultaneously optimize the design and operation of the process in response to variable power loads and volatile electricity prices. We consider a carbon capture system that is integrated with a natural gas combined cycle (NGCC) power plant. An ionic liquid (IL) that chemically absorbs  ${\rm CO}_2$  is used as the solvent. ILs have been identified as promising alternatives to aqueous amine solvents due to their superior properties such as lower heats of absorption and negligible volatility (Ramdin et al., 2012; Aghaie et al., 2018). To account for long-term variation in plant load and electricity prices, we present a scenario-based optimization problem. Subsequently, we evaluate the behavior and costs of the optimal flexible carbon capture process and compare the results with a reference inflexible process.

## 2. $CO_2$ capture process flowsheet model

Fig. 1 depicts a carbon capture process. It involves an absorption section and a solvent regeneration section that includes a flash tank. In the absorption section, CO2 is chemically absorbed in the IL solvent in a packed-bed absorption column. An intercooling system is used to enhance absorption efficiency. The CO2-rich solvent is preheated using hot CO2-lean solvent, and then enters the flash tank for regeneration. The source of energy for solvent regeneration is steam extracted from the low-pressure (LP) turbine of a power plant. By reducing the steam diverted for solvent regeneration, more steam can be used for power generation, which can increase the electricity output. For flexible operation, the carbon capture system can adjust solvent regeneration to optimize energy consumption and allow for more power generation as needed. Finally, the captured CO2 is compressed for storage or further use. In this study, the IL triethyl-(octyl)phosphonium 2-cyanopyrrolide ([P<sub>2228</sub>][2-CNPyr]) is used as the chemical solvent due to its favorable properties including high absorption capacity, moderate reaction enthalpy, superior reversibility, and relatively low viscosity (Seo et al., 2014). This IL belongs to the class of aprotic heterocyclic anion (AHA) ILs. AHA ILs incorporate an amine functionality in the anion, which contains azolide-type ring structures (Gurkan et al., 2010). The unique structure of AHA ILs enables equimolar chemical absorption of CO2 while maintaining high reversibility. One notable advantage is that the viscosities of AHA ILs do not increase significantly after reaction with CO2. This is attributed to the absence of free protons in AHA anions,

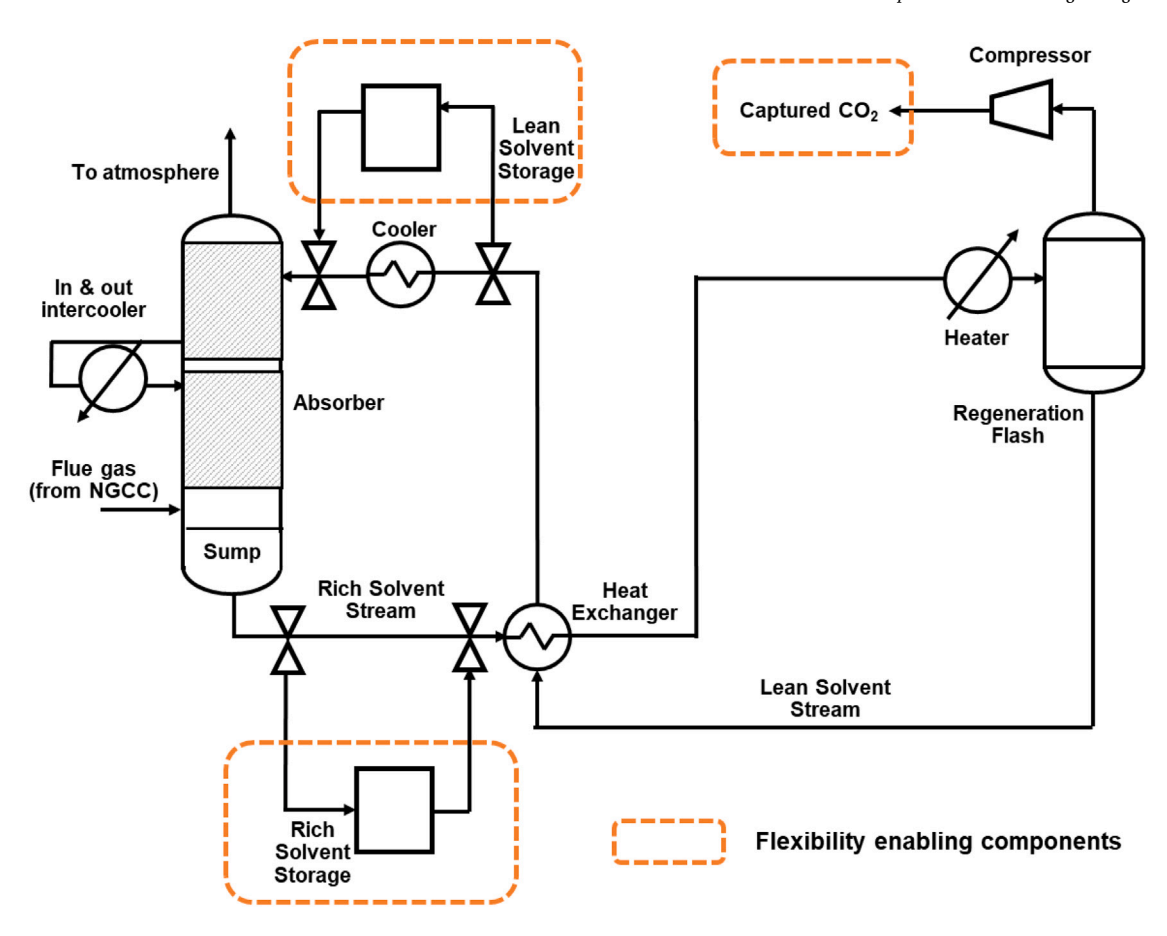


Fig. 1. Schematic diagram of IL-based carbon capture process. Solvent storage tanks and variable capture rate are used to enable flexibility.

which prevents the formation of hydrogen-bonding networks after the reaction with CO2.

To allow for flexible operation, the process utilizes both variable capture levels and solvent storage tanks. The capture level can be selectively reduced (in general, during peak hours) by lowering either the regeneration temperature or the amount of solvent being regenerated. This results in a significant reduction in energy consumption for solvent regeneration and  ${\rm CO}_2$  compression during this period. Solvent regeneration can also be delayed during peak electricity demand/prices by storing the rich solvent in a tank. The CO2-rich solvent from the absorber can be stored to reduce the energy consumption required for regeneration and compression, allowing the power plant to maximize electricity output by reducing the steam flow extracted from the LP turbine of the NGCC. Additionally, CO2-lean solvent from the lean solvent tank can be used to allow for full load CO2 capture while deferring the energy consumption for regeneration.

In this paper, we introduce a dynamic model of an IL-based carbon capture plant based on the steady-state model developed in our previous work (Seo et al., 2020). For the sake of brevity, we focus on presenting the new models (specifically, the process dynamics and the model for the storage systems) in this section. The complete flowsheet model including the IL thermophysical properties (Seo et al., 2020), rate-based absorber model (Seo et al., 2020), and heat exchanger model (Seo et al., 2021) can be found in our previous work.

## 2.1. Absorber dynamic model

The mass and energy balances for the absorber are represented considering the dynamics of the time-varying liquid hold-up volume, as represented by the equations (Walters et al., 2016a):

$$\frac{1}{Z_{\text{abs}}S} \frac{\partial \left(F^{\text{V}} y_i\right)}{\partial z} = -N_i^{\text{V}}, \quad i = \text{CO}_2, \text{N}_2, \text{O}_2$$
 (1)

$$\sum y_i = 1, \quad i = CO_2, N_2, O_2$$
 (2)

$$\sum_{\substack{\partial \left(\varepsilon_{\mathrm{L}}C_{i}^{\mathrm{L}}\right) \\ \partial t}} y_{i} = 1, \quad i = \mathrm{CO}_{2}, \mathrm{N}_{2}, \mathrm{O}_{2} \tag{2}$$

$$\frac{\partial \left(\varepsilon_{\mathrm{L}}C_{i}^{\mathrm{L}}\right)}{\partial t} + \frac{1}{Z_{\mathrm{abs}}S} \frac{\partial \left(F^{\mathrm{L}}x_{i}\right)}{\partial z} = N_{i}^{\mathrm{L}}, \quad i = \mathrm{CO}_{2}, \mathrm{IL} \tag{3}$$

$$\sum x_i = 1, \quad i = \text{CO}_2, \text{ IL}$$
 (4)

where z is the normalized axial position and  $Z_{\rm abs}$  and S are the height and cross-sectional area of the column, respectively.  $F^{V}$  and  $F^{L}$  are the vapor and liquid molar flowrates, and  $y_i$  and  $x_i$  represent the vapor and liquid phase mole fractions for component i.  $\varepsilon_{\rm L}$  is the liquid hold-up in the packing and  $C_i^L$  is the molar density for component i. Note that molar hold-up in the vapor phase is much smaller than in the liquid phase, so the vapor phase dynamics are assumed to be negligible (Walters et al., 2016a).  $N_i$  refers to the molar transfer rates (per unit volume of bed) of each component i. The overall mass transfer coefficient can be derived based on the gas and liquid phase mass transfer resistances, accounting for the enhanced mass transfer rate due to chemical reaction between  ${\rm CO}_2$  and IL (Seo et al., 2020). An in-and-out intercooling system is implemented mid-way to minimize the impact of heat from the exothermic CO2 absorption reaction. The semi-rich IL solvent is drawn off at the bottom of the upper packing section. After passing through the intercooler, the semi-rich solvent is then returned to the top of the lower packing section. In addition to the liquid holdup in the packing, a first-order linear response is assumed to account for substantial liquid holdup in the absorber sump (Walters et al., 2016b). We assume that the absorber sump has a residence time of  $\tau = 5$  min. This allows us to capture the behavior of this unit over time, accounting for the time that elapses between changes in input streams and their effects on the output streams:

$$\tau \frac{\partial \chi_{\text{sump,out}}}{\partial t} = \chi_{\text{sump,in}} - \chi_{\text{sump,out}}$$
 (5)

where  $\chi_{\text{sump,in}}$  and  $\chi_{\text{sump,out}}$  are the relevant inlet and outlet stream properties including enthalpy and component mole fractions.

#### 2.2. Regeneration flash unit dynamic model

The regeneration flash unit is described by the following material and energy balances:

$$L_{\text{flash,in}} = L_{\text{flash,out}} + V_{\text{flash,out}} \tag{6}$$

$$x_{i,\text{flash,in}} L_{\text{flash,in}} = x_{i,\text{flash,out}} L_{\text{flash,out}} + y_{i,\text{flash,out}} V_{\text{flash,out}}, \quad i = \text{CO}_2, \text{ IL}$$
(7)

$$H_{\rm flash,in}L_{\rm flash,in} = H_{\rm flash,out}^{\rm L}L_{\rm flash,out} + H_{\rm flash,out}^{\rm V}V_{\rm flash,out} - Q \tag{8}$$

where  $L_{\rm in}$  is the inlet liquid flowrate and  $V_{\rm flash,out}$  and  $L_{\rm flash,out}$  represent the molar flowrates of vapor and liquid leaving the flash tank, respectively.  $x_{\mathrm{flash,in}}$ , and  $x_{\mathrm{flash,out}}$  denote the molar fractions of the inlet and outlet streams in liquid phase, and  $y_{\rm flash,out}$  denotes the molar fraction of the outlet streams in vapor phase.  $H_{\mathrm{flash,in}}$ ,  $H_{\mathrm{flash,out}}$  are the molar enthalpies of the inlet and outlet streams of the flash tank. Q is the heat duty required for regenerating the IL solvent. Similar to the absorber sump, a simple dynamic model is used to represent tank dynamics. This model also assumes first-order response with a time constant of 5 min (Walters et al., 2016b):

$$\tau \frac{\partial \chi_{\text{flash,out}}}{\partial t} = \chi_{\text{flash,in}} - \chi_{\text{flash,out}}$$
 (9)

where  $\chi_{\text{flash,in}}$  and  $\chi_{\text{flash,out}}$  represent the inlet and outlet stream properties of the flash unit.

#### 2.3. Solvent storage tank model

The overall mass and heat balances for the solvent storage tanks are given by:

$$\frac{\partial M}{\partial t} = L_{\rm in} - L_{\rm out} \tag{10}$$

$$\frac{\partial (Mx_{i,\text{storage}})}{\partial t} = L_{\text{in}}x_{i,\text{in}} - L_{\text{out}}x_{i,\text{out}} \quad i = \text{CO}_2, \text{ IL}$$
(11)

$$\frac{\partial M}{\partial t} = L_{\rm in} - L_{\rm out}$$

$$\frac{\partial (Mx_{i,\rm storage})}{\partial t} = L_{\rm in}x_{i,\rm in} - L_{\rm out}x_{i,\rm out} \quad i = \rm CO_2, \, IL$$

$$\frac{\partial (MH_{\rm storage})}{\partial t} = L_{\rm in}H_{\rm in} - L_{\rm out}H_{\rm out}$$
(12)

where M represents the total number of moles of liquid in the tank,  $L_{\rm in}$  and  $L_{\rm out}$  are the molar flow rates of the input and output streams, and  $x_{\rm storage},~x_{\rm in},$  and  $x_{\rm out}$  are the  ${\rm CO_2}$  mole fractions of the liquid in storage, and in the input and output streams, respectively. Similarly,  $H_{\text{storage}}$ ,  $H_{\text{in}}$ , and  $H_{\text{out}}$  are the molar enthalpies of the stored material, and inlet and outlet streams, respectively. The equations assume that the tank is well-mixed, and that there are no reactions or phase change taking place.

## 3. Optimization problem formulation

In this section we present an optimization framework used to simultaneously make both design and operational decisions for the carbon capture plant under fluctuations in power load and consequently in electricity prices. Electricity prices and the power plant load are considered as uncertain parameters and are represented through a set of scenarios.

## 3.1. Variable power loads and electricity prices

Fig. 2 shows the selected dataset for three representative scenarios considered in this work. We use day-ahead electricity market prices in Texas (Electric Reliability Council of Texas, 2022) and output data from Wolf Hollow II power station (an NGCC power plant, located in Granbury, Texas) (United States Environmental Protection Agency, 2022). Texas was selected as a representative location because wind and solar account for over 20% of the electricity generation within

Flue gas composition for case B31B (James et al., 2019).

Flue gas component	Value (mole%)		
Ar	0.89		
CO <sub>2</sub>	4.08		
H <sub>2</sub> O	8.75		
$N_2$	74.28		
$O_2$	12.00		

the local independent system operator (ERCOT) (United States Energy Information Administration, 2022b) and therefore influence electricity prices significantly. We assume that the power plant can operate at or below its capacity (1231 MW), without completely shutting down. The power plant output varies on a daily basis in response to the grid demand. Note that the locational marginal price of electricity on the power grid can experience significant fluctuations under certain circumstances, such as extreme weather conditions that may cause many power-generating units to go offline, thereby disrupting the electricity supply. An example of such a case is scenario 2, in which there is an extremely high excursion in the electricity price during peak hours. However, the probability of such events causing extreme volatility in price is generally low.

The feed composition of the flue gas, as shown in Table 1, is considered to be constant and equal to that reported in the DOE baseline case B31B (NGCC plant with a net output of 646 MW) (James et al., 2019). We assume that water present in the flue gas is removed from the flue gas during a pretreatment dehydration process (the cost of dehydration is not considered). This precapture dehydration offers several advantages. Firstly, it reduces the overall flow rate entering the downstream carbon capture process, resulting in smaller equipment sizes, lower capital costs, and reduced utility duties. Secondly, removing water at this stage helps mitigate issues such as corrosion and hydrate formation, which can lead to additional costs and complications. Additionally, other species in the flue gas apart from CO2, such as N2 and O2, are considered inert and it is assumed that they are not absorbed by the IL, based on experimental findings indicating negligible absorption (Bennett, 2014; Anthony et al., 2005; Lei et al., 2014; Song et al., 2019).

## 3.2. Cost evaluation

In this study, we perform an economic evaluation of a carbon capture plant considering detailed capital and operating costs. The capital cost estimation includes the absorber, heat exchanger, storage tanks, solvent cooler, regeneration heater, and compressor costs. The operating cost includes expenses related to regeneration heating, cooling, gas conveyance by blower, and compression.

The capital cost is annualized based on the purchased equipment cost (PEC), as suggested in Frailie (2014):

Total annualized capital cost (\$/year) = 
$$\alpha \times \beta \times PEC$$
 (\$), (13)

where  $\alpha$  is a scaling factor that converts PEC to total capital cost and includes direct cost, indirect cost, and working capital, and  $\beta$  is the factor that annualizes capital cost and addresses return on investment, tax, depreciation, and maintenance. We use the values of 5 and 0.2 for the scaling and annualization factors, respectively, as suggested by Lin and Rochelle (2014). We also consider the cost of solvent startup, which is assumed to be 10 dollars/kg (Mota-Martinez et al., 2018). We summarize key correlation models in Tables 2 and 3.

For CO<sub>2</sub> compression, to account for the increased capacity needed to accommodate increased CO2 flow when the extra solvent is being regenerated, a compressor with variable speed drive is used. The frequency supplied to the drive motor is regulated based on compression load. Therefore, the motor can operate at a reduced speed and consume less energy during reduced load (Lüdtke, 2004). This type of

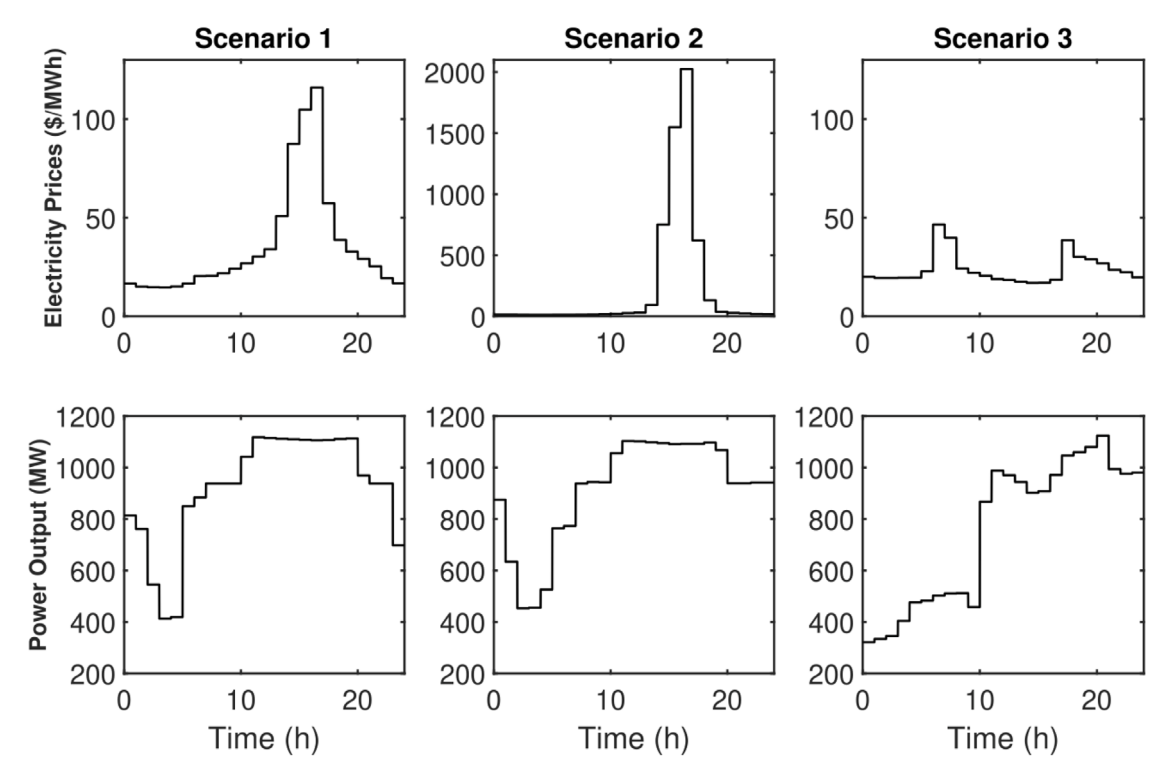


Fig. 2. Day ahead electricity prices (Electric Reliability Council of Texas, 2022) and power output of the NGCC power station (United States Environmental Protection Agency, 2022). Case 1: moderate, Case 2: high, Case 3: low variability in electricity prices.

compressor can handle a maximum allowable load of 105% of its design capacity (Stewart, 2018). To determine the appropriate size for the compressor, we first obtain the maximum load during compression over the operating hours, which is 100% of the compressor's design capacity. We then size the compressor based on the base load. For solvent cooling, a cost of \$0.354/GJ for cooling ( $\geq$  30 °C) (Turton et al., 2012) and \$4.43/GJ for refrigeration ( $\geq$  15 °C) are used. The regeneration cost is calculated based on the equivalent electrical work, which accounts for the electricity output penalty due to steam extraction from the power plant (shown in Eq. (30)).

## 3.3. Scenario-based optimization under uncertainty

The scenario-based optimization formulation minimizing the overall cost for carbon capture is represented as:

$$\min_{d,z} \sum_{k \in \Omega} \frac{1}{t_f} \left( w_k \int_0^{t_f} f_k \left( d, x_k(t), z_k(t), \theta_k(t) \right) dt \right)$$
s.t. carbon capture plant dynamic model operating constraints (33)

where the objective function is the expected annualized cost based on weighted 24 h operation costs for the scenarios considered. f represents process costs (including capital, operating, and solvent inventory costs) and is weighted by the probability of each scenario occurring in long-term operation (represented by the scenario weight,  $w_k$ ). k refers to the scenarios considered, and  $\Omega$  denotes the set of scenarios. d and z are, respectively, the process design variables (e.g., sizes of unit operations) and the operating variables (e.g., flowrates, temperature) being optimized.  $x_k$  are process variables and  $\theta_k$  are time-varying parameters that represent fluctuations in energy prices and flue gas load. As depicted in Fig. 3, time-varying parameters and process operating decisions are treated as piecewise constant, with intervals of one hour. The process design variables remain fixed over time.

In this study, three specific days in 2020 were chosen as representative of high, moderate, and low variability scenarios in electricity prices (shown in Fig. 2). The power plant outputs from the same days are used for the corresponding load variation in each scenario. The scenario weights  $(w_k)$  are determined by calculating the Euclidean distance between the electricity prices of each selected day and all the remaining days in 2020. The corresponding scenario weights for high, moderate, and low variability cases are 0.0082, 0.3224, and 0.6694, respectively, based on ERCOT electricity price data from 2020.

The operating constraints implemented for inflexible and flexible operation are shown in Table 4. In both cases, the heat exchanger temperature approach must be at least 1 °C (Eqs. (35) and (38)) and the maximum regeneration temperature is 150 °C (Eqs. (36) and (39)) (to avoid solvent degradation) throughout the entire time horizon. We note that the thermal stability of an IL will depend on the specific choice of the anion, cation, and their substituents. Long-term stability studies are require to determine the process operating constraints for a specific IL choice. A detailed study of the thermal stability of a large number of ILs has been provided recently by Huang et al. (2021) who find that the thermal stability of ILs is influenced significantly by the choice of cation and anion, as well as the specific gaseous environment. Thus, the upper limit on the regeneration temperature may need to be modified depending on the circumstances. For the inflexible operation mode, the CO2 removal rate is kept at a minimum of 90% throughout the entire time horizon (Eq. (34)) and the storage tanks are not utilized. In contrast, the flexible operation mode allows for adjustments in the CO<sub>2</sub> capture level over time, while ensuring that the time-average removal is at least 90% over the 24 h horizon (Eq. (37)). In addition, constraints are imposed to ensure that the solvent cannot flow into and out of a storage tank at the same time (Eq. (40)). The inventory levels in the lean and rich solvent storage tanks must be at least at their initial values by the end of the time horizon (Eq. (41)). Solvent inventory levels are constrained to be between 20% and 80% of the storage tank volume (Eq. (42)) to ensure efficient and safe operation to prevent operation disruptions such as potential overfilling.

Table 2
Purchased equipment costs.

Equipment	Correlation		Description	Source
	$S = \frac{\pi D_{\text{packing}}^2}{4}$ $C_{\text{packing}} = (6.36a_{\text{p}} + 176.6) \left(\frac{\pi D_{\text{packing}}^2}{4} Z_{\text{abs}}\right)$	(14) (15)	S: cross-sectional area of the packing, $D_{\text{packing}}$ : diameter of the packing, $a_p$ : specific area of the packing, $Z_{\text{abs}}$ : height of the packing section,	
Packed column	$\begin{split} W_{\text{shell}} &= \frac{\pi}{4} L \left( (D_{\text{packing}} + t h_{\text{metal}})^2 - D_{\text{packing}}^2 \right) \rho_{\text{metal}} \\ C_{\text{shell}} &= 518.2 (W_{\text{shell}})^{0.609} \\ C_{\text{manhole}} &= 3,480 \ Z_{\text{abs}} \\ C_{\text{distributors}} &= 11/6 \left( 13,350 D_{\text{packing}}^{0.176} \right) \\ C_{\text{auxiliaries}} &= 985.33 \ D_{\text{packing}} + 759.33 \\ \text{PEC}_{\text{column}}(\$) &= C_{\text{packing}} + C_{\text{shell}} + C_{\text{manhole}} + C_{\text{distributors}} + C_{\text{auxiliaries}} \end{split}$	(16) (17) (18) (19) (20) (21)	$th_{\mathrm{metal}}$ : thickness of the metal shell, $\rho_{\mathrm{metal}}$ : density of the metal, $W_{\mathrm{shell}}$ : weight of the metal shell, $C_{\mathrm{packing}}$ : cost of the packing, $C_{\mathrm{shell}}$ : cost of the metal shell, $C_{\mathrm{manhole}}$ : cost of the manhole, $C_{\mathrm{distributors}}$ : cost of the liquid distributors, $C_{\mathrm{auxilliaries}}$ : cost of the auxiliaries. PEC_{column} represents the purchased equipment cost of the packed column.	Tsai (2010)
Storage tank	$PEC_{flash}(\$) = 264.172 V_{storage}^{0.51}$	(22)	$V_{ m storage}$ represents the volume of the storage tank in cubic meters. PEC $_{ m flash}$ represents the purchased equipment cost of the storage tank.	Seider et al. (2009)
Solvent cooler	$PEC_{cooler}(\$) = 22.16A$	(23)	$A$ represents the heat transfer area of the solvent cooler in square feet. $PEC_{cooler}$ represents the purchased equipment cost of the solvent cooler.	Tsay et al. (2019)
Regeneration heater <sup>a</sup>	$\begin{split} &C_{\rm B} = \exp(11.0545 - 0.9228 \ln(A_{\rm ref}) + \\ &0.0986 \left[ \ln(A_{\rm ref}) \right]^2) \\ &F_{\rm M} = 1.75 + \left( \frac{A_{\rm ref}}{100} \right)^{0.13} \\ &F_{\rm p} = 0.9803 + 0.018 \left( \frac{P}{100} \right) + 0.0017 \left( \frac{P}{100} \right)^2 \\ &{\rm PEC}_{\rm heater}(S) = \frac{A}{A_{\rm ref}} F_{\rm M} F_{\rm P} C_{\rm B} \end{split}$	(24) (25) (26) (27)	$A$ represents the heat transfer area of the regeneration heater in square feet. $A_{\rm ref}$ represents the reference heat transfer area. $P$ represents the pressure of the system in kPa. $C_{\rm B}$ represents the base cost. $F_{\rm M}$ and $F_{\rm p}$ are material factor and tube-length correlation, respectively. PEC <sub>heater</sub> represents the purchased equipment cost of the heater.	Seider et al. (2009)
Heat exchanger	PEC <sub>heat exchanger</sub> (\$) = 22.16A	(28)	A represents the heat transfer area of the heat exchanger in square feet. PEC <sub>heat exchanger</sub> represents the purchased equipment cost of the heat exchanger.	Tsay et al. (2019)
CO <sub>2</sub> compressor	$PEC_{\text{compressor}}(\$) = M_{\text{CO}_2}^{\forall} \left( -2.05 \ln(P) + 0.17 \ln P^2 + 6.76 \right)$	(29)	$P$ represents the regeneration pressure in bar. $M_{\text{CO}_2}^{\text{V}}$ represents the amount of CO <sub>2</sub> captured in tons. PECcompressor represents the purchased equipment cost of the CO <sub>2</sub> compressor.	Lin and Rochelle (2014)

 $<sup>{}^{</sup>a}A_{ref}$  is 12,000 ft<sup>2</sup>.

Table 3
Electric equivalent work for steam heating, gas blower, compressor, and pump.

Equipment	Correlation		Source
Heating <sup>a</sup>	$W_{ m heating}({ m MW}) = \eta_{ m turbine} \left(rac{T_{ m steam} - T_{ m sink}}{T_{ m steam}} ight) Q_{ m heating}$	(30)	Lin and Rochelle (2014)
Gas blower <sup>b</sup>	$W_{ m blower}({ m MW}) = rac{G^V \Delta P}{10^6 \eta_{ m blower}}$	(31)	Tsai (2010)
CO <sub>2</sub> compressor <sup>c</sup>	$W_{\text{compressor}}(kW) = F_{\text{CO}_{3}}^{V}(-3.48\ln(P) + 14.85)$	(32)	Lin (2016)

<sup>&</sup>lt;sup>a</sup>Turbine efficiency,  $\eta_{\text{turbine}}$  is assumed to be 0.9.  $T_{\text{steam}}$  and  $T_{\text{sink}}$  are fixed to 160 and 38 °C, respectively.  $Q_{\text{heating}}$  is regeneration heat duty.

## 4. Results and discussion

The model described above has ~6,000 equations and the optimization problem is solved using the NLPSQP solver in gPROMS ProcessBuilder and within 15 h of CPU time on a 64-bit Windows 10 PC equipped with an Intel Core i7 processor running at 3.20 GHz and 16.0 GB RAM. We note that the solver used will return a local minimum. The process variables are bounded within physically feasible bounds throughout the time horizon. This avoids solutions that are physically infeasible, such as negative molar fractions, pressures, areas, or velocities, while providing some degree of flexibility in the system. However, it is possible that alternative solutions may exist. Global optimization strategies such as a reduced-spaced formulation approach (Bongartz and Mitsos, 2019) could be used, but this is beyond the scope of this work. We believe that this could be an important direction for future work.

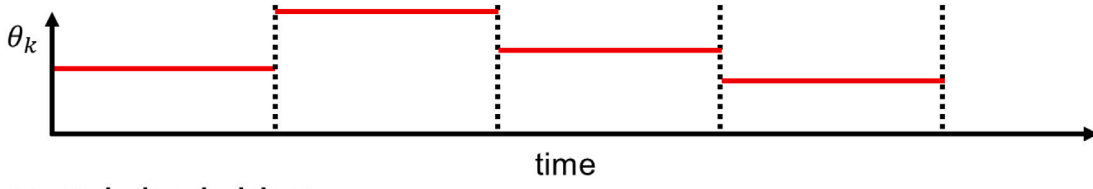
We analyze the optimal design and operation of a carbon capture system, focusing on the impact of providing flexibility in the carbon capture system. The results are compared to those of a case without flexibility, where the carbon capture rate is kept constant (90%) and solvent storage tanks are not utilized.

Table 5 provides the optimum values for key design and operational variables for the carbon capture process, showing the differences between the flexible and inflexible operation modes. In flexible operation, the optimal diameter of the column packing for the absorber is larger to accommodate the increased (intermittent) liquid flowrates due to the utilization of the storage system. The lean solvent tank is used to provide solvent (to the absorber) while the rich solvent tank stores solvent (from the absorber) during peak hours. This behavior is reversed during off-peak hours. The maximum inventory level in each tank can vary due to the influence of system dynamics. The maximum flows to and from storage decrease when there is less fluctuation in the electricity prices. With the smallest price fluctuation (scenario 3), the nominal 90% overall carbon capture rate is achieved mainly by adjusting the instantaneous capture level and regeneration duty, making the use of solvent storage less important. However, for moderate and high price

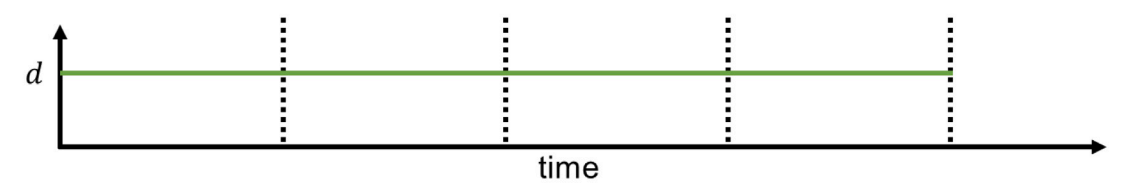
<sup>&</sup>lt;sup>b</sup>Blower efficiency,  $\eta_{\text{blower}}$  is assumed to be 0.75.  $\Delta P$  is the total pressure drop in Pa.  $G^V$  is the feed gas flowrate in cubic meters per second.

 $<sup>{}^{\</sup>rm c}P$  is the regeneration pressure in bar.  $F_{{\rm CO}_2}^{\rm V}$  is molar flowrate of  ${\rm CO}_2$  compressed in moles per sec.

# Time-varying inputs



# Process design decisions



# Process operating decisions

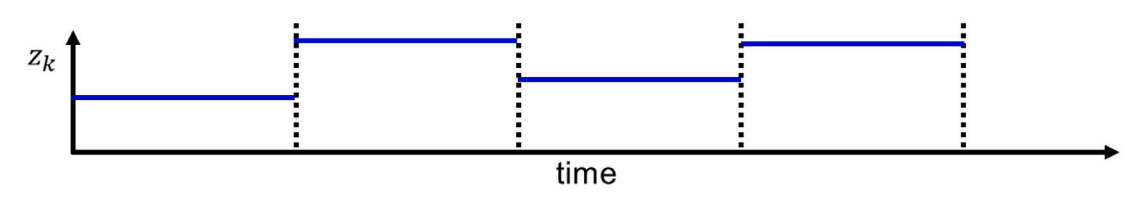


Fig. 3. Schematic illustrations of time-varying parameters, process design variables, and process operating variables over time.

Table 4
A summary of decision variables and process constraints for the optimization problem.

Component	Relevant variables and equations	
Inflexible operation		
Decision variables	$F^{\rm L}$ , $Z_{ m abs}$ , $D$ , $T_{ m absorber}$ , $T_{ m intercooling}$ , $T_{ m heat}$ exchanger,hot,out, $T_{ m regeneration}$ $\frac{F^{\rm V}_{{\rm CO}_2,m}-F^{\rm V}_{{\rm CO}_2,m}}{F^{\rm V}_{{\rm CO}_2,m}} \geq 0.9 \ \forall t$	(34)
Process constraints	$\Delta T_{\text{appr, min}} \ge 1 ^{\circ}\text{C} \forall t$	(35)
	$T_{\text{regeneration}} \leq 150 ^{\circ}\text{C}  \forall t$	(36)
Flexible operation		
Decision variables	$Z_{ m abs},~D,~T_{ m absorber},~T_{ m intercooling},~T_{ m heat}~{ m exchanger,hot,out},~T_{ m regeneration},$	
	$\begin{array}{l} L_{\rm rich,in}, \ L_{\rm rich,out}, \ L_{\rm lean,in}, \ L_{\rm lean,out} \\ \frac{\int_0^{t_f} F_{\rm CO_2,in}^{\rm C} dt - \int_0^{t_f} F_{\rm CO_2,out}^{\rm V} dt}{\int_0^{t_f} F_{\rm CO_2,in}^{\rm V} dt} \geq 0.9 \end{array}$	(37)
	$\Delta T_{\text{appr, min}} \ge 1 ^{\circ}\text{C}  \forall t$	(38)
Process constraints	$T_{\text{regeneration}} \leq 150 ^{\circ}\text{C} \forall t$	(39)
	$L_{ ext{storage,in}}L_{ ext{storage,out}}=0 \ orall t$	(40)
	$M(t_f) - M(t_0) \ge 0$	(41)
	$0.2V_{\text{storage}} \leq V_{\text{solvent inventory}} \leq 0.8V_{\text{storage}} \ \forall t$	(42)

**Table 5**Optimal values of key process design and operation variables.

Decision variables	Inflexible	Flexible	Lower bound	Upper bound
Absorber packing height (m)	15.06	14.88	2	40
Absorber diameter (m)	22.8	25.9	1	100
Rich solvent storage max inlet flowrate $[k = 1]$ (kmol/s)	_	0.86	0	10
Rich solvent storage max inlet flowrate $[k = 2]$ (kmol/s)	-	1.20	0	10
Rich solvent storage max inlet flowrate $[k = 3]$ (kmol/s)	-	0.45	0	10
Lean solvent storage max outlet flowrate $[k = 1]$ (kmol/s)	_	0.84	0	10
Lean solvent storage max outlet flowrate $[k = 2]$ (kmol/s)	_	1.57	0	10
Lean solvent storage max outlet flowrate $[k = 3]$ (kmol/s)	_	0.37	0	10
Rich solvent storage capacity (m <sup>3</sup> )	_	26,813	0	50,000
Lean solvent storage capacity (m <sup>3</sup> )	-	23,332	0	50,000

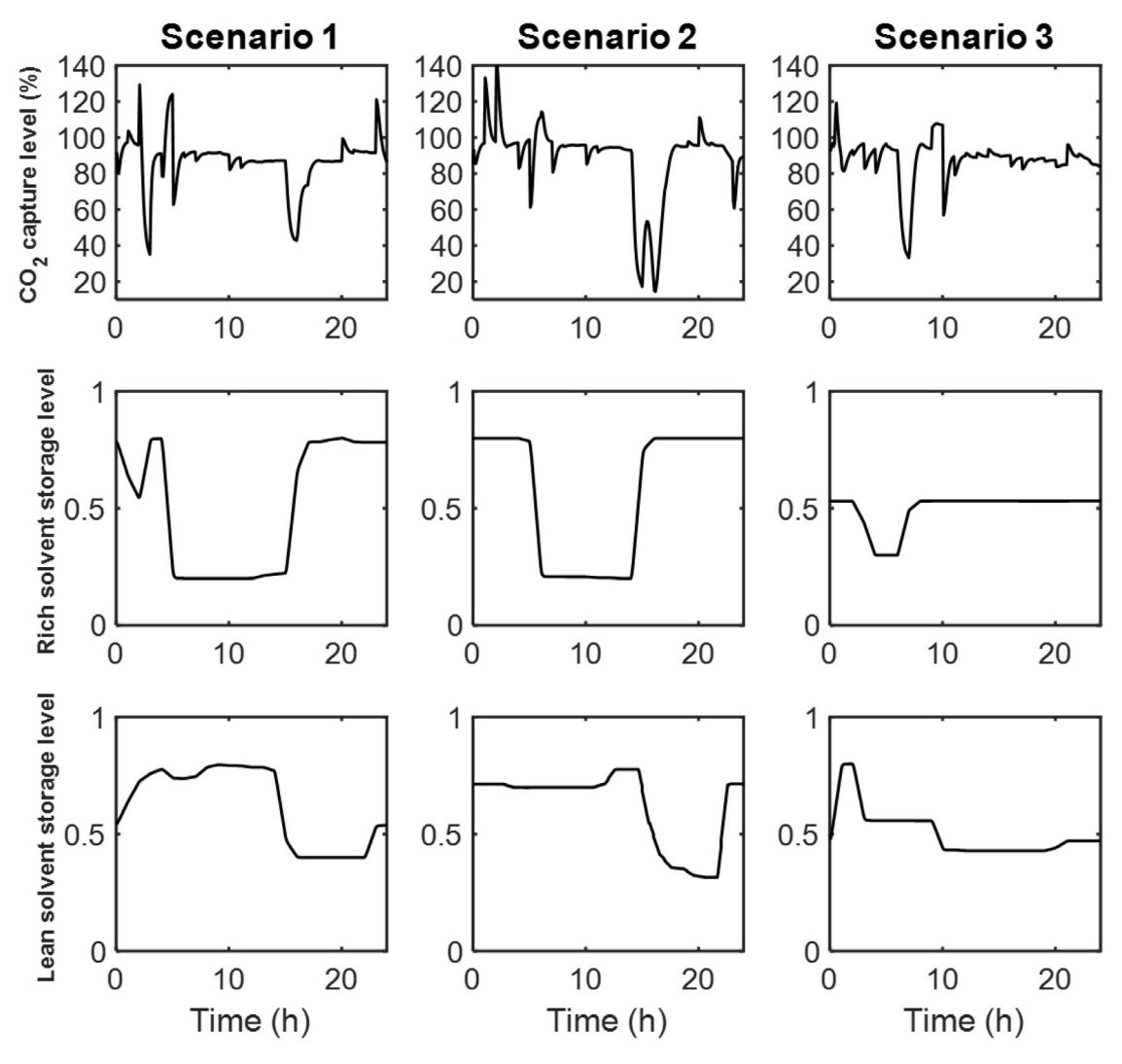


Fig. 4. Optimized instantaneous CO2 capture level, rich solvent storage level, and lean solvent storage level.

variability scenarios (scenarios 1 and 2), solvent storage becomes more important.

Fig. 4 shows the optimal time-varying CO2 capture levels and storage tank levels as a function of time for each scenario. The corresponding solvent flowrates and CO2 concentrations in the rich-CO2 solvent are show in Fig. 5. Note that the overall (time-average) CO2 capture level over 24 h of operation is maintained at 90% for all cases, while the instantaneous capture level (the instantaneous percentage of CO2 captured related to CO2 feed) may exceed 100% due to system dynamics and intermittent replenishment and/or consumption of rich and lean solvent inventory. The instantaneous capture rate is minimized during the peak electricity price hours of t = 14 to 16 h for the moderate (k = 1) and high (k = 2) price variation scenarios, and t = 6to 8 h for the low variation scenario (k = 3). During periods of lower electricity cost, the instantaneous capture rate increases to compensate. In general, a more substantial variation in instantaneous capture rate is observed when there is a larger fluctuation in electricity prices, as alluded to above. This variation can be achieved by reducing regeneration temperature or storing (thus delaying regeneration of) CO2-rich solvent (Fig. 5). The CO2-rich solvent is stored during peak electricity price hours for the moderate (k = 1) and high (k = 2) variation scenarios. The stored rich solvent is regenerated when the electricity price is relatively low and power plant load is reduced (t = 4 to 6 h). The solvent inventory levels at the end of the time horizon returns to their starting values (see constraints in Table 5). It is important to

emphasize that the strategies employed in this work (variable capture level and the use of storage tanks) provide greater advantages in achieving the target capture level (overall 90%) compared to the option of flue gas bypassing. These strategies allow for the delay of regeneration during peak hours while maintaining continuous CO2 capture while the bypassing option completely bypasses the CO2 capture. There is relatively little usage of storage in the low variation scenario (k = 3). In this scenario, the instantaneous capture rate increases when the power plant operates at lower output (0-6 h, 9-10 h). Therefore, modulating the capture level is sufficient to compensate for peak demand when the power plant operates at lower capacity and when the electricity price fluctuations are small. These results indicate that it would be more efficient to use the storage tanks when the power plant load is high and when the electricity price fluctuations are significant (storage level changes significantly). For the low variation scenario, adjusting the instantaneous capture level can be a more cost-effective solution than relying on storage tanks.

Fig. 6 compares the regeneration temperature for inflexible and flexible operation. In the inflexible case, the capture rate is 90% at all times. In addition, since the storage tanks are not used, the liquid circulation rates are constant. Therefore, the regeneration process follows *power load* patterns, and the regeneration temperature for the inflexible case is similar to the load pattern shown in Fig. 2. On the other hand, flexible operation offers a more malleable approach. Regeneration temperature responds to *electricity prices* to minimize the heat

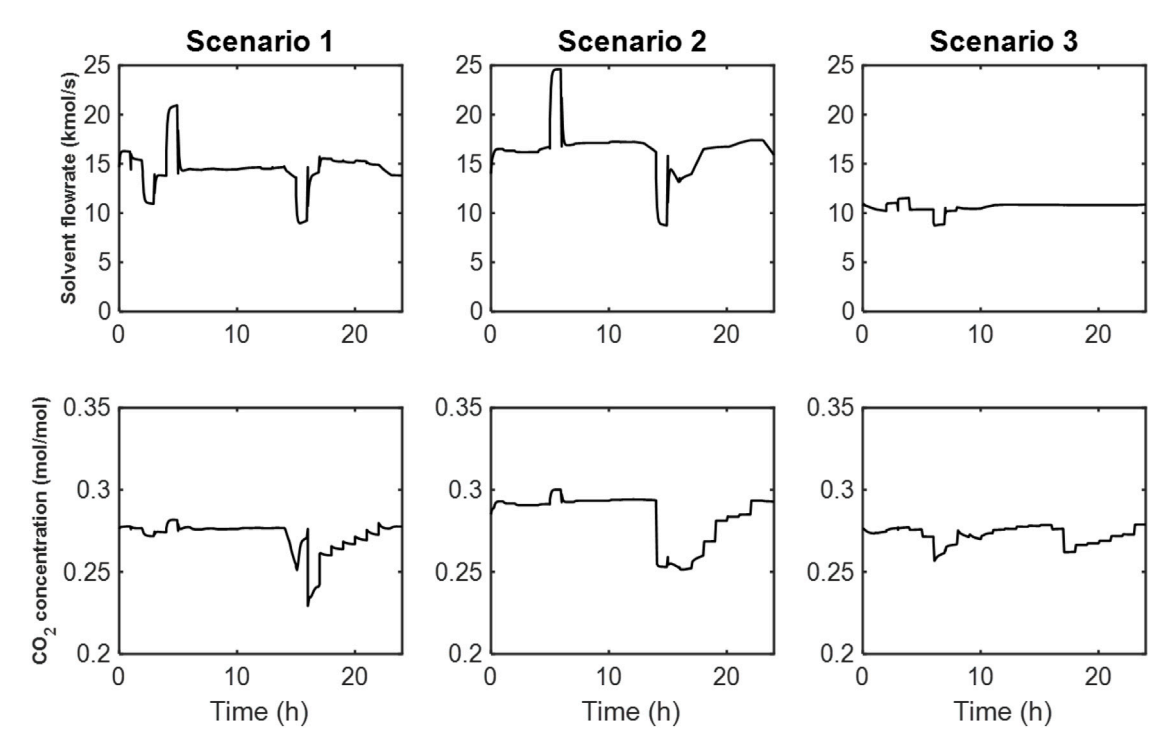


Fig. 5. Optimized solvent flowrate and CO<sub>2</sub> concentration of the CO<sub>2</sub>-rich stream from regeneration flash.

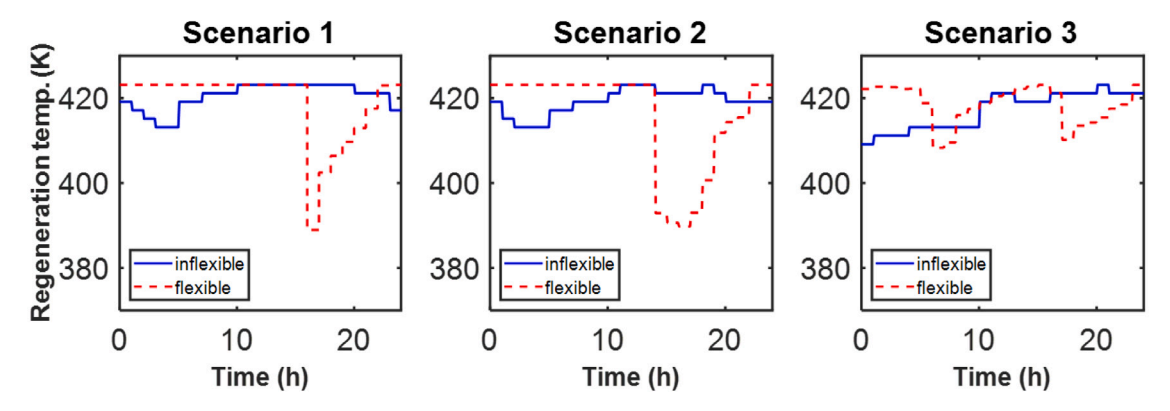


Fig. 6. Optimized regeneration temperature for inflexible (blue solid lines) and flexible (red dashed lines) operations.

duty required for regeneration during peak times. The instantaneous capture rate is variable in this case, and the lean solvent inventory can be used to temporarily compensate for the less lean solvent (higher  $\rm CO_2$  loading in the lean solvent) from the lower-temperature regeneration. This flexibility offers a more cost-efficient solution.

We note that while electricity prices have an impact on some of the operating variables, there are elements that are not affected by fluctuations in electricity prices. As an example, Fig. 7 shows the optimized blower work for inflexible and flexible operation. Although the operating cost of blower is dependent on electricity prices, the blower work does not vary in response to electricity prices. This is primarily because the blower work is determined by the flue gas feed flowrate (Eq. (31)), which is a function of power plant load (note that we do not allow bypassing of the flue gas because it is difficult to achieve a reduction in overall  $\mathrm{CO}_2$  emissions from the process). Therefore, the blower work follows the plant load pattern rather than electricity price variations, leading to similar operating patterns for both inflexible and flexible operation.

Table 6 and Fig. 8 show the optimal results for the annualized capital, solvent inventory, and operating costs. In comparison to the inflexible operation case (which has no solvent storage tanks and a

constant capture rate), the flexible operation has a 3.6% higher optimized annualized capital cost. This is mainly due to the larger size of the absorber, heat exchanger and compressor, and the addition of the storage tanks (which increases both solvent storage and solvent inventory costs). The overall annualized process cost is reduced by 3.7% in the flexible case as compared to the inflexible one. This saving can mainly be attributed to the avoidance of regeneration and compression during periods of high electricity prices.

The results show that the total cost savings for each scenario, as compared to the inflexible scenario, are 3.6%, 17.8%, and 0.02%. These findings suggest that a flexible operation would be especially effective in situations with significant renewable energy penetration. However, when the load and electricity variation is relatively low, it may not be worthwhile to implement a storage system, as this would lead to additional costs for solvent storage and inventory.

## 5. Conclusions

As the contribution of variable renewable energy (VRE) to the power generation mix increases, dispatchable power plants must make frequent output changes to meet changes in energy demand and VRE

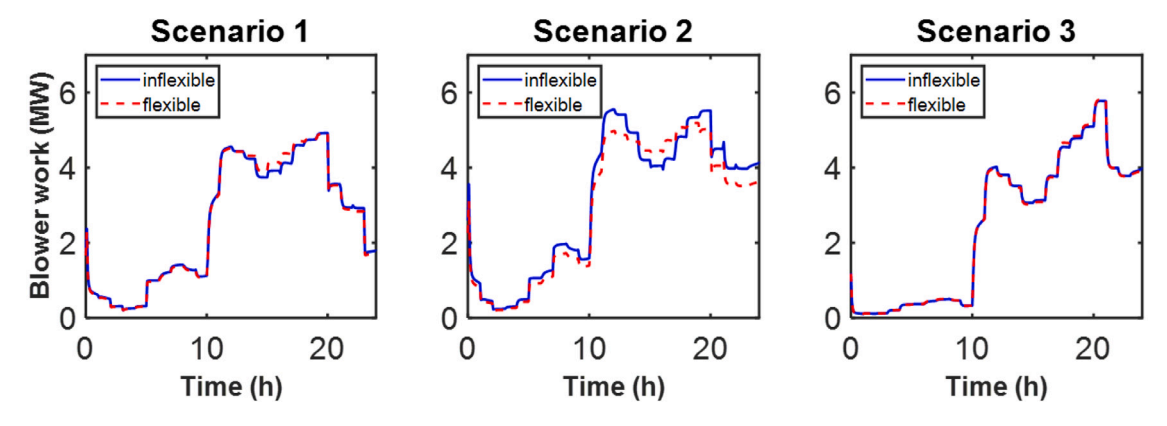


Fig. 7. Optimized blower work for inflexible (blue solid lines) and flexible (red dashed lines) operations.

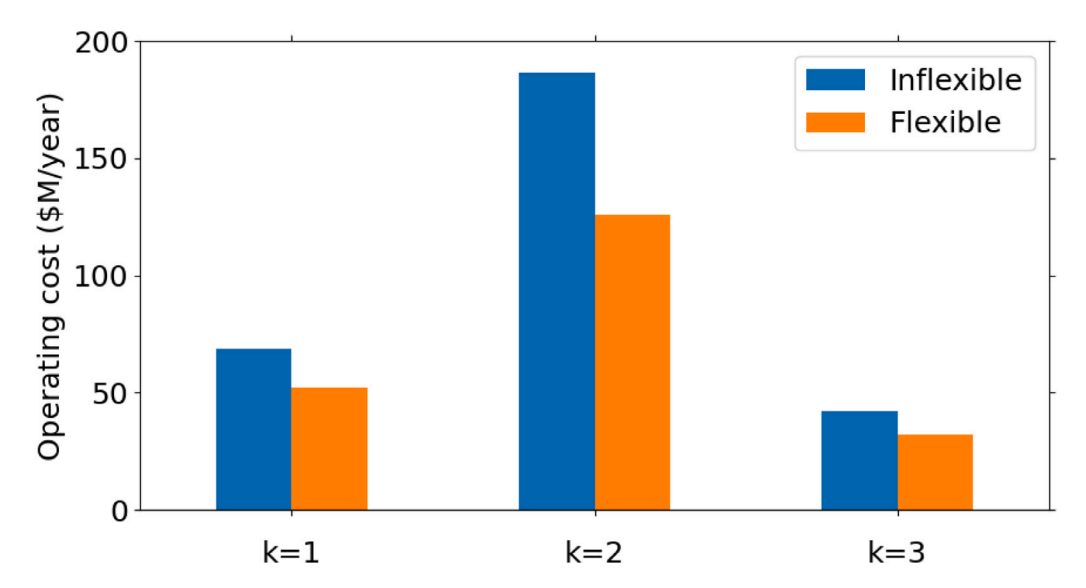


Fig. 8. Optimized process operating costs for inflexible (left) and flexible (right) operation.

Table 6
Optimized process costs.

	Inflexible		flexible			
	k = 1	k = 2	k = 3	k = 1	k = 2	k = 3
Capital cost item			Annualized c	ost (\$M/year)		
Absorber		40.7			41.2	
Heat exchanger		10.2			10.5	
Compressor		19.5			20.9	
Pump		1.6			1.6	
Blower		1.7			1.7	
Cooler		8.2			8.3	
Heater		12.1			12.3	
Storage		-			0.9	
Operating cost item						
Heating	43.5	122.5	23.6	30.2	76.3	16.5
Total cooling	12.1	18.0	9.0	12.3	17.8	8.3
Total electricity	13.0	46.2	9.6	9.8	32.0	7.3
CAPEX	94.0			97.4		
OPEX	68.6	186.7	42.2	52.3	126.1	32.1
Solvent (initial startup + storage inventory)	4.1	3.9	3.8	11.0	10.5	10.3
Total cost	166.7	284.6	140.1	160.7	234.0	139.8

supply. Additionally, electricity prices are inherently volatile due to varying supply and demand balances. To mitigate large electricity cost penalties resulting from such fluctuations, flexible operation of carbon capture plants should be considered.

In this study, we propose a dynamic optimization formulation that simultanesouly consider the design and operation of a flexible carbon capture plant that utilizes ian ionic liquid solvent. We introduce flexible operating components such as solvent storage and variable carbon capture rate to enable flexible operation. We use a scenario-based stochastic optimization framework that evaluates the performance of flexible carbon capture by optimizing the process design and operation of a carbon capture system connected to a natural gas combined cycle (NGCC) power plant. While, for illustration purposes, a set of scenarios is used to represent variations in electricity price and power load at a specific location, the framework is general. Optimal design and operational variables are simultaneously obtained for each scenario set. The analysis considers capital and operating costs, including absorption, heat exchange, storage, regeneration, and compression systems.

The results provide optimal design and operating conditions for a carbon capture plant in response to load and electricity price fluctuations. The findings demonstrate that flexible carbon capture systems offer operational flexibility to the system by temporarily decoupling CO<sub>2</sub> absorption and solvent generation to avoid high regeneration and compression costs during high load and demand periods. The study shows that flexible operation provides significant economic savings over the inflexible operation, as it combines the advantages of both capture level reduction and solvent storage. The benefits of flexibility can vary depending on the specific circumstances of operation. In general, flexible operation can mitigate the effects of intermittent load and electricity prices and reduce costs related to regeneration and compression. Regeneration rates track electricity prices while blower works track power load. However, it is important to note that there may be situations where the costs of implementing a storage system and operating in flexible mode outweigh the potential benefits. In such cases, it may be more cost-effective to use flexible operation without a storage system, particularly if power demand and electricity prices are relatively stable.

## CRediT authorship contribution statement

**Kyeongjun Seo:** Methodology, Software, Investigation, Visualization, Writing – original draft. **Adhika P. Retnanto:** Writing – original draft. **Jorge L. Martorell:** Writing – original draft. **Thomas F. Edgar:** Supervision. **Mark A. Stadtherr:** Supervision, Investigation, Writing – review & editing. **Michael Baldea:** Conceptualization, Funding acquisition, Investigation, Supervision, Writing – review & editing.

## Declaration of competing interest

The authors declare that they have no conflicts of interest.

## Data availability

Data will be made available on request.

## Acknowledgments

The authors gratefully acknowledge the financial support provided by ExxonMobil through the Fueling a Sustainable Energy Transition (FSET) program of the University of Texas at Austin Energy Institute. KS was partially supported by the Phillips 66 Fellowship and the Graduate School Continuing Fellowship at the University of Texas. Partial financial support from the National Science Foundation under the ECO CBET award 2133543 is also acknowledged.

#### References

- Aghaie, M., Rezaei, N., Zendehboudi, S., 2018. A systematic review on CO<sub>2</sub> capture with ionic liquids: Current status and future prospects. Renew. Sustain. Energy Rev. 96, 502–525. http://dx.doi.org/10.1016/j.rser.2018.07.004.
- Alie, C., Elkamel, A., Douglas, P.L., Croiset, E., 2016. Reduced-order modelling of flexible CCS and assessment using short-term resource scheduling approach. Int. J. Greenhouse Gas Control 48, 253–274. http://dx.doi.org/10.1016/j.ijggc.2016. 01.025.
- Anthony, J.L., Anderson, J.L., Maginn, E.J., Brennecke, J.F., 2005. Anion effects on gas solubility in ionic liquids. J. Phys. Chem. B 109 (13), 6366–6374. http://dx.doi.org/10.1021/jp046404l.
- Bennett, J.E., 2014. Acid Gas and Nitrogen Solubility in Ionic Liquids for Carbon Capture Applications (Ph.D. thesis). The University of Notre Dame, URL https://curate.nd.edu/show/6h440r98709.
- Bongartz, D., Mitsos, A., 2019. Deterministic global flowsheet optimization: Between equation-oriented and sequential-modular methods. AIChE J. 65, 1022–1034. http: //dx.doi.org/10.1002/aic.16507.
- Bruce, A.R.W., Gibbins, J., Harrison, G.P., Chalmers, H., 2016. Operational flexibility of future generation portfolios using high spatial- and temporal-resolution wind data.
   IEEE Trans. Sustain. Energy 7 (2), 697–707. http://dx.doi.org/10.1109/TSTE.2015.
   2497704
- Bui, M., Adjiman, C.S., Bardow, A., Anthony, E.J., Boston, A., Brown, S., Fennell, P.S., Fuss, S., Galindo, A., Hackett, L.A., Hallett, J.P., Herzog, H.J., Jackson, G., Kemper, J., Krevor, S., Maitland, G.C., Matuszewski, M., Metcalfe, I.S., Petit, C., Puxty, G., Reimer, J., Reiner, D.M., Rubin, E.S., Scott, S.A., Shah, N., Smit, B., Trusler, J.P.M., Webley, P., Wilcox, J., Mac Dowell, N., 2018. Carbon capture and storage (CCS): The way forward. Energy Environ. Sci. 11, 1062–1176. http://dx.doi.org/10.1039/C7EE02342A.
- Bui, M., Gunawan, I., Verheyen, V., Feron, P., Meuleman, E., Adeloju, S., 2014. Dynamic modelling and optimisation of flexible operation in post-combustion CO<sub>2</sub> capture plants—A review. Comput. Chem. Eng. 61, 245–265. http://dx.doi.org/10.1016/j. compchemeng.2013.11.015.
- Chalmers, H., Lucquiaud, M., Gibbins, J., Leach, M., 2009. Flexible operation of coal fired power plants with postcombustion capture of carbon dioxide. J. Environ. Eng.-Asce 134, 449–458. http://dx.doi.org/10.1016/j.ijggc.2019.04.023.
- Cheng, F., Patankar, N., Chakrabarti, S., Jenkins, J.D., 2022. Modeling the operational flexibility of natural gas combined cycle power plants coupled with flexible carbon capture and storage via solvent storage and flexible regeneration. Int. J. Greenhouse Gas Control 118, 103686. http://dx.doi.org/10.1016/j.ijggc.2022.103686.
- Cohen, S.M., Rochelle, G.T., Webber, M.E., 2011. Optimal operation of flexible post-combustion CO<sub>2</sub> capture in response to volatile electricity prices. Energy Procedia 4, 2604–2611. http://dx.doi.org/10.1016/j.egypro.2011.02.159, 10th International Conference on Greenhouse Gas Control Technologies.
- Cohen, S.M., Webber, M.E., Rochelle, G.T., 2012. The Impact of Electricity Market Conditions on the Value of Flexible CO<sub>2</sub> Capture. In: ASME International Mechanical Engineering Congress and Exposition, vol. 6, pp. 581–593. http://dx.doi.org/10. 1115/IMECE2012-88119.
- Electric Reliability Council of Texas, 2022. Day-ahead price. http://www.ercot.com/. Errey, O., Chalmers, H., Lucquiaud, M., Gibbins, J., 2014. Valuing responsive operation of post-combustion CCS power plants in low carbon electricity markets. Energy Procedia 63, 7471–7484. http://dx.doi.org/10.1016/j.egypro.2014.11.784, 12th International Conference on Greenhouse Gas Control Technologies, GHGT-12.
- Frailie, P.T., 2014. Modeling of Carbon Dioxide Absorption/Stripping by Aqueous Methyldiethanolamine/Piperazine (Ph.D. thesis). The University of Texas at Austin.
- Gonzalez-Salazar, M.A., Kirsten, T., Prchlik, L., 2018. Review of the operational flexibility and emissions of gas- and coal-fired power plants in a future with growing renewables. Renew. Sustain. Energy Rev. 82, 1497–1513. http://dx.doi. org/10.1016/j.rser.2017.05.278.
- Gurkan, B., Goodrich, B., Mindrup, E., Ficke, L., Massel, M., Seo, S., Senftle, T., Wu, H., Glaser, M., Shah, J., Maginn, E., Brennecke, J., Schneider, W., 2010. Molecular design of high capacity, low viscosity, chemically tunable ionic liquids for CO<sub>2</sub> capture. J. Phys. Chem. Lett. 1, 3494–3499. http://dx.doi.org/10.1021/jz101533k.
- Hao, P., Singh, S., Liu, X., Tian, Y., Ku, A.Y., 2020. Flexible CO<sub>2</sub> capture in China. Int. J. Greenhouse Gas Control 101, 103140. http://dx.doi.org/10.1016/j.ijggc.2020. 103140
- Hou, Q., Zhang, N., Du, E., Miao, M., Peng, F., Kang, C., 2019. Probabilistic duck curve in high PV penetration power system: Concept, modeling, and empirical analysis in China. Appl. Energy 242, 205–215. http://dx.doi.org/10.1016/j.apenergy.2019. 03.067.
- Huang, Y., Chen, Z., Crosthwaite, J.M., N.V.K. Aki, S., Brennecke, J.F., 2021. Thermal stability of ionic liquids in nitrogen and air environments. J. Chem. Thermodyn. 161, 106560. http://dx.doi.org/10.1016/j.jct.2021.106560.
- James, R.E., Kearins, D., Turner, M., Woods, M., Kuehn, N., Zoelle, A., 2019. Cost and Performance Baseline for Fossil Energy Plants Volume 1: Bituminous Coal and Natural Gas to Electricity. Tech. Rep. NETL-PUB-22638, U.S. Department of Energy, http://dx.doi.org/10.2172/1569246.
- Jockenhoevel, T., Schneider, R., Rode, H., 2009. Development of an economic post-combustion carbon capture process. Energy Procedia 1 (1), 1043–1050. http://dx.doi.org/10.1016/j.egypro.2009.01.138, Greenhouse Gas Control Technologies 9.

- Kárászová, M., Zach, B., Petrusová, Z., Červenka, V., Bobák, M., Šyc, M., Izák, P., 2020. Post-combustion carbon capture by membrane separation, review. Sep. Purif. Technol. 238, 116448. http://dx.doi.org/10.1016/j.seppur.2019.116448.
- Khalilpour, R., 2014. Multi-level investment planning and scheduling under electricity and carbon market dynamics: Retrofit of a power plant with PCC (post-combustion carbon capture) processes. Energy 64, 172–186. http://dx.doi.org/10.1016/j. energy 2013 10 086
- Lei, Z., Dai, C., Chen, B., 2014. Gas solubility in ionic liquids. Chem. Rev. 114 (2), 1289–1326. http://dx.doi.org/10.1021/cr300497a.
- Lin, Y.-J., 2016. Modeling Advanced Flash Stripper for Carbon Dioxide Capture Using Aqueous Amines (Ph.D. thesis). The University of Texas at Austin, URL http: //hdl.handle.net/2152/41988.
- Lin, Y.-J., Rochelle, G.T., 2014. Optimization of advanced flash stripper for CO<sub>2</sub> capture using piperazine. Energy Procedia 63, 1504–1513. http://dx.doi.org/10.1016/j.egypro.2014.11.160, 12th International Conference on Greenhouse Gas Control Technologies, GHGT-12.
- Lüdtke, K.H., 2004. Process Centrifugal Compressors. PennWell Books.
- Mota-Martinez, M.T., Brandl, P., Hallett, J.P., Mac Dowell, N., 2018. Challenges and opportunities for the utilisation of ionic liquids as solvents for  $CO_2$  capture. Mol. Syst. Des. Eng. 3, 560–571. http://dx.doi.org/10.1039/C8ME00009C.
- Plaza, J.M., Wagener, D.V., Rochelle, G.T., 2009. Modeling CO<sub>2</sub> capture with aqueous monoethanolamine. Energy Procedia 1 (1), 1171–1178. http://dx.doi.org/10. 1016/j.egypro.2009.01.154, URL https://www.sciencedirect.com/science/article/pii/S1876610209001556, Greenhouse Gas Control Technologies 9.
- Ramdin, M., Loos, T., Vlugt, T., 2012. State-of-the-art of CO<sub>2</sub> capture with ionic liquids. Ind. Eng. Chem. Res. 51, 8149–8177. http://dx.doi.org/10.1021/ie3003705.
- Rochelle, G., Chen, E., Freeman, S., Van Wagener, D., Xu, Q., Voice, A., 2011. Aqueous piperazine as the new standard for  $\mathrm{CO}_2$  capture technology. Chem. Eng. J. 171 (3), 725–733. http://dx.doi.org/10.1016/j.cej.2011.02.011.
- Rúa, J., Bui, M., Nord, L.O., Mac Dowell, N., 2020. Does CCS reduce power generation flexibility? A dynamic study of combined cycles with post-combustion CO<sub>2</sub> capture. Int. J. Greenhouse Gas Control 95, 102984. http://dx.doi.org/10.1016/j.ijggc.2020. 102984.
- Rubin, E.S., Chen, C., Rao, A.B., 2007. Cost and performance of fossil fuel power plants with CO<sub>2</sub> capture and storage. Energy Policy 35 (9), 4444–4454. http://dx.doi.org/10.1016/j.enpol.2007.03.009.
- Samanta, A., Zhao, A., Shimizu, G.K.H., Sarkar, P., Gupta, R., 2012. Post-combustion CO<sub>2</sub> capture using solid sorbents: A review. Ind. Eng. Chem. Res. 51 (4), 1438–1463. http://dx.doi.org/10.1021/ie200686q.
- Seider, W.D., Lewin, D.R., Seader, J.D., Widagdo, S., Gani, R., Ng, K.M., 2009. Product and Process Design Principles: Synthesis, Analysis, and Evaluation, third ed. John Wiley & Sons, Inc.
- Seo, K., Chen, Z., Edgar, T.F., Brennecke, J.F., Stadtherr, M.A., Baldea, M., 2021. Modeling and optimization of ionic liquid-based carbon capture process using a thin-film unit. Comput. Chem. Eng. 155, 107522. http://dx.doi.org/10.1016/j. compchemeng.2021.107522.
- Seo, S., Quiroz-Guzman, M., DeSilva, M.A., Lee, T.B., Huang, Y., Goodrich, B.F., Schneider, W.F., Brennecke, J.F., 2014. Chemically tunable ionic liquids with aprotic heterocyclic anion (AHA) for  $\rm CO_2$  capture. J. Phys. Chem. B 118 (21), 5740–5751. http://dx.doi.org/10.1021/jp502279w.
- Seo, K., Tsay, C., Hong, B., Edgar, T.F., Stadtherr, M.A., Baldea, M., 2020. Rate-based process optimization and sensitivity analysis for ionic-liquid-based post-combustion carbon capture. ACS Sustain. Chem. Eng. 8, 10242–10258. http://dx.doi.org/10.1021/acssuschemeng.0c03061.

- Song, T., Morales-Collazo, O., Brennecke, J.F., 2019. Solubility and diffusivity of oxygen in ionic liquids. J. Chem. Eng. Data 64 (11), 4956–4967. http://dx.doi.org/10. 1021/acs.jced.9b00750.
- Spitz, T., González Díaz, A., Chalmers, H., Lucquiaud, M., 2019. Operating flexibility of natural gas combined cycle power plant integrated with post-combustion capture. Int. J. Greenhouse Gas Control 88, 92–108. http://dx.doi.org/10.1016/j.ijggc.2019. 04.023
- Stewart, M., 2018. Surface Production Operations. Gulf Professional Publishing.
- Tsai, R.E., 2010. Mass Transfer Area of Structured Packing (Ph.D. thesis). The University of Texas at Austin, URL http://hdl.handle.net/2152/ETD-UT-2010-05-1412.
- Tsay, C., Pattison, R.C., Zhang, Y., Rochelle, G.T., Baldea, M., 2019. Rate-based modeling and economic optimization of next-generation amine-based carbon capture plants. Appl. Energy 252, 113379. http://dx.doi.org/10.1016/j.apenergy.2019. 113379.
- Turton, R., Bailie, R.C., Whiting, W.B., Shaeiwitz, J.A., Bhattacharyya, D., 2012.
  Analysis, Synthesis and Design of Chemical Processes, fourth ed. Prentice Hall, pp. 203–230.
- United States Energy Environmental Protection Agency, 2023. Inventory of U.S. greenhouse gas emissions and sinks. URL https://www.epa.gov/ghgemissions/inventory-us-greenhouse-gas-emissions-and-sinks.
- United States Energy Information Administration, 2022a. Annual Energy Outlook 2022.

  Tech. Rep., URL https://www.eia.gov/outlooks/aeo/pdf/AEO2022\_ChartLibrary\_full.pdf.
- United States Energy Information Administration, 2022b. State electricity profiles. https://www.eia.gov/electricity/state/texas/.
- United States Environmental Protection Agency, 2022. Air markets program data. https://ampd.epa.gov/ampd/.
- Walters, M.S., Edgar, T.F., Rochelle, G.T., 2016a. Dynamic modeling and control of an intercooled absorber for post-combustion  $\mathrm{CO}_2$  capture. Chem. Eng. Process. Process Intens. 107, 1–10. http://dx.doi.org/10.1016/j.cep.2016.05.012.
- Walters, M.S., Edgar, T.F., Rochelle, G.T., 2016b. Regulatory control of amine scrubbing for CO<sub>2</sub> capture from power plants. Ind. Eng. Chem. Res. 55 (16), 4646–4657. http://dx.doi.org/10.1021/acs.iecr.6b00318.
- Wu, X., Yu, Y., Qin, Z., Zhang, Z., 2014. The advances of post-combustion CO<sub>2</sub> capture with chemical solvents: Review and guidelines. Energy Procedia 63, 1339–1346. http://dx.doi.org/10.1016/j.egypro.2014.11.143, 12th International Conference on Greenhouse Gas Control Technologies, GHGT-12.
- Zaman, M., Lee, J.H., 2015. Optimization of the various modes of flexible operation for post-combustion CO<sub>2</sub> capture plant. Comput. Chem. Eng. 75, 14–27. http: //dx.doi.org/10.1016/j.compchemeng.2014.12.017.
- Zanco, S.E., Pérez-Calvo, J.-F., Gasós, A., Cordiano, B., Becattini, V., Mazzotti, M., 2021. Postcombustion  $CO_2$  capture: A comparative techno-economic assessment of three technologies using a solvent, an adsorbent, and a membrane. ACS Eng. Au 1 (1), 50–72. http://dx.doi.org/10.1021/acsengineeringau.1c00002.
- Zantye, M.S., Arora, A., Faruque Hasan, M., 2019. Operational power plant scheduling with flexible carbon capture: A multistage stochastic optimization approach. Comput. Chem. Eng. 130, 106544. http://dx.doi.org/10.1016/j.compchemeng.2019. 106544.
- Zantye, M.S., Arora, A., Hasan, M.M.F., 2021. Renewable-integrated flexible carbon capture: A synergistic path forward to clean energy future. Energy Environ. Sci. 14, 3986–4008. http://dx.doi.org/10.1039/D0EE03946B.